The tensor-entanglement renormalization group of the 2D quantum rotor model

Rolando La Placa
Department of Physics, Harvard University, Cambridge, MA, 02138
(Dated: May 16, 2014)

We review the tensor-renormalization group (TRG)[1], and the tensor-entanglement renormalization group (TERG) [2]. Then, we use TERG to setup a variational optimization of the ground state of the $O(2)$ quantum rotor model in a square lattice.

I. INTRODUCTION

Tensor-renormalization group (TRG) is a real-space renormalization technique used to study any 2-dimensional classical lattice systems with local interactions [1]. It stems from the idea that any such system can be rewritten as a tensor-network model. To describe a tensor-network model, we assign a p-rank tensor $T_{ij\dots}$ to every site of a lattice, where p- is the number of bonds in each site. Each index $\{i, j, \dots\}$ is D dimensional, and can be seen as residing on an adjacent bond of the site (Fig. 1). For a classical lattice model Hamiltonian $-\beta H = -\beta H(i, j, \dots)$ with local interactions, we can find a tensor T such that

$$Z = \sum_{i,j,\dots} e^{-\beta H(i,j,\dots)} = \sum_{i,j,\dots} T_{ijkl} T_{emfg} \cdots . \qquad (1)$$

A real space-renormalization transformation $T \to T'$ can be carried out to study the critical behavior of tensor-network models.

Motivated by the classical-quantum mapping in which the partition function of a d-dimensional quantum model can be mapped to the partition function of a $d+1$ dimensions classical model, we expect that a similar renormalization technique to be valid in the study of some 1-dimensional quantum systems. In fact, examples of TRG-based calculations for the quantum spin-1/2 and spin-1 chains can be found in Ref. [3].

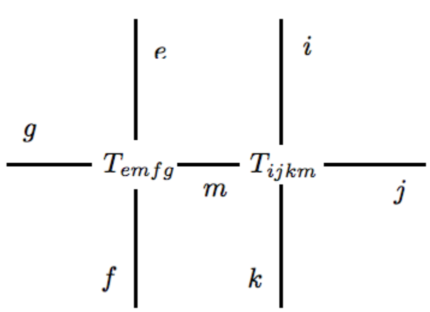

FIG. 1. A Tensor-network model on a square lattice.

Additionally, tensor-networks models and TRG can be used to perform variational calculations. Traditional mean-field theory cannot be applied in systems with long-range entanglement, such as phases found beyond Landau's symmetry breaking paradigm [2]. In some cases, "Tensor Product States" (TPS) are possible trial ground state wave functions. To define a TPS, consider a system with quantum numbers $m_i \in 1, 2, \dots, M$ residing over a square lattice. A TPS of this square lattice is

$$|\Psi(\{m_i\})\rangle = \sum_{i,j\dots} T^{m_1}_{ijkm} T^{m_2}_{emfg} \cdots \qquad (2)$$

where $T^{m_i}_{ijkm}$ are complex numbers, $\{m_i\}$ are the physical M-dimensional indexes, and $\{i, j, \dots\}$ are the indexes with bond dimensionality D. The bond dimensionality might vary according to the model being studied, e.g. $D = 2$ is enough to reproduce the quantum Ising model, and the Heisenberg model [2]. Using a TPS as a ground state ansatz,

$$\frac{\langle\Psi|H|\Psi\rangle}{\langle\Psi|\Psi\rangle} \geq 0 \qquad (3)$$

can be minimized to find the appropriate tensor components. This is computationally hard, but TRG can be used to reduce the complexity of the computation.

This variational approach using TPS and TRG can be seen as an attempt to generalized the variational optimization described by the "Matrix Product States" (MPS) and the density matrix renormalization group (DMRG). DMRG has been an effective method to study 1-dimensional models such as spin chains [4]. In Section III, we will discuss a TRG-based method called the tensor-entanglement renormalization group (TREG). TERG is an approximation scheme to perform the variational calculation described above. Finally, we try to use TERG on the 2-dimensional $O(2)$ quantum rotor lattice.

II. TENSOR-ENTANGLEMENT RENORMALIZATION GROUP

Given a translationally invariant Hamiltonian on a lattice with sites α and local interactions, $H = \sum_\alpha H_\alpha$, we will try an ansatz for the ground state in the form of shown in Eq. 2. By assumptions, H_α can be written in terms of local operators: $H_\alpha = O^{\alpha,0} + O^{\alpha,1}O^{\beta,2} + \cdots$.

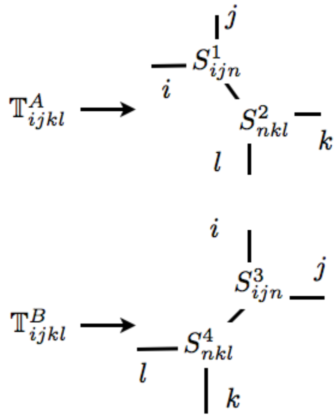

FIG. 2. Decomposition of a 4-tensor into two 3-tensors. For sublattice A , we decompose into S^1 and S^2. In sublattice B, the decomposition is into S^3 and S^4.

Which means that we can rewrite:

$$\begin{aligned}\langle\Psi|\Psi\rangle &= \sum_{m_1,\ldots,ii',jj',\ldots} T^{m_1}_{ijkm}\overline{T}^{m_1}_{i'j'k'm'}T^{m_2}_{emfg}\overline{T}^{m_2}_{e'm'f'g'}\cdots \\ &= tTr[\mathbb{T}\otimes\mathbb{T}\otimes\cdots]\end{aligned} \quad (4)$$

$$\begin{aligned}\langle\Psi|H_\alpha|\Psi\rangle &= \sum_{m_1,\ldots,ii',jj',\ldots} O^{\alpha,0}_{m_1m_2}T^{m_1}_{ijkm}\overline{T}^{m_1}_{i'j'k'm'}T^{m_2}_{emfg}\cdots \\ &+ \sum_{m_1,\ldots,ii',jj',\ldots} O^{\alpha,1}_{m_1m_2}O^{\beta,2}_{m_2m_3}T^{m_1}_{ijkm}\overline{T}^{m_1}_{i'j'k'm'}T^{m_2}_{emfg}\cdots+\cdots \\ &= tTr[\mathbb{T}^{\alpha,0}\otimes\mathbb{T}\cdots]+tTr[\mathbb{T}^{\alpha,1}\otimes\mathbb{T}^{\beta,2}\otimes\mathbb{T}\cdots]+\cdots\end{aligned} \quad (5)$$

The tensor trace denotes summation over all indices, and we have defined $\mathbb{T}=\sum_m \overline{T}^m\otimes T^m$ and $\mathbb{T}^{\alpha,a}=\sum_{k,k'} O^{\alpha,a}_{kk'}\overline{T}^k\otimes T^{k'}$ with $O^{\alpha,a}_{kk'}$ being the (k,k') matrix element of $O^{\alpha,a}$ in the basis of quantum numbers k. Calculating the tensor traces is computationally expensive, but with the real-space renormalization we can decimate the tensor lattice and find an approximation with less degrees of freedom. We will find $\tilde{\mathbb{T}}$ s.t.

$$tTr[\mathbb{T}\otimes\mathbb{T}\otimes\cdots]\approx tTr[\tilde{\mathbb{T}}\otimes\tilde{\mathbb{T}}\otimes\cdots] \quad (6)$$

with the tensor trace over $\tilde{\mathbb{T}}$ containing one-fourth of the tensors in $tTr[\mathbb{T}\otimes\mathbb{T}\otimes\cdots]$. This approximation transformations $\mathbb{T}\to\tilde{\mathbb{T}}$ is based on TRG [1].

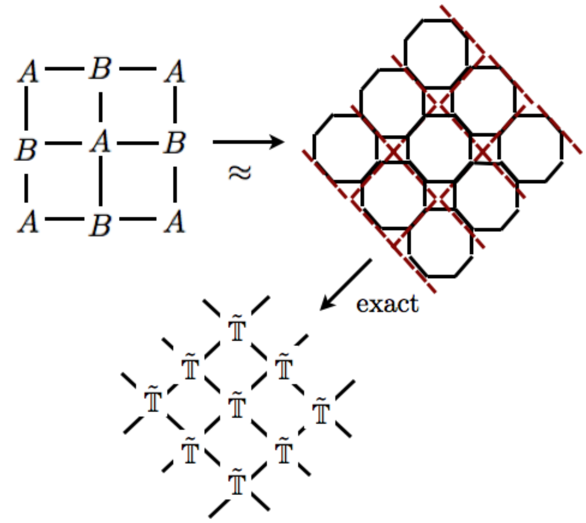

FIG. 3. Tensor-renormalization transformation of a square lattice.

Start by dividing the square lattice into two sublattices A and B as shown in Fig. 3. Then, decompose the tensors $\mathbb{T}$ at each site of A sublattice in terms of two 3-rank tensors S^1 and S^2, and do a similar decomposition of tensors in the B sublattice into 3-rank tensors S^3 and S^4 (Fig. 2). Note that the $\mathbb{T}$ tensors can be seen as 4-rank tensors in which each index has D^2 dimensions. We have

$$\mathbb{T}^A_{ijkl}=\sum_n S^1_{ijn}S^2_{nkl}, \quad (7)$$
$$\mathbb{T}^B_{ijkl}=\sum_n S^3_{ijn}S^4_{nkl}$$

with i,j,k,l each having D^2 dimensions and n being D^4-dimensional. With an approximation, we can reduce the dimensionality of n. Viewing $\mathbb{T}^A_{ijkl}$ as a matrix $M^A_{ij;kl}$, we can factorize it into its singular value decomposition (SVD), $M^A_{ij;kl}=U^A_{ij,n}\Lambda^A_{n,n'}V^{A\dagger}_{n',kl}$. Finally, we approximate M by only considering the biggest D_c singular values λ_n. Letting $S^1_{ijn}=\sqrt{\lambda_n}U^A_{ij,n}$ and $S^2_{nkl}=\sqrt{\lambda_n}V^{A\dagger}_{n,kl}$ so that the approximate decomposition becomes.

$$\mathbb{T}^A_{ijkl}\approx\sum_n^{D_c} S^1_{ijn}S^2_{nkl}. \quad (8)$$

The same process is done with the B sublattice. After this transformation we end up with lattice of the form shown in Fig. 3. By adding the degrees of freedom found in each small square in the new 3-rank tensors S lattice (see Fig. 4), we obtain the desired $\tilde{\mathbb{T}}$

$$\tilde{\mathbb{T}}_{qrst}=\sum_{i,j,k,l} S^1_{jkq}S^2_{rli}S^3_{ijs}S^4_{tkl}. \quad (9)$$

By our SVD approximation, the tensor $\tilde{\mathbb{T}}_{qrst}$ has indexes of D_c dimensions, and the transformation gives us

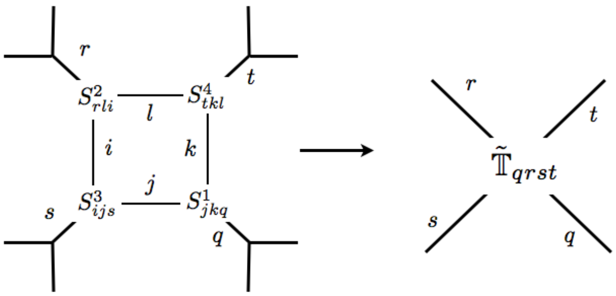

FIG. 4. Adding the S tensors in a square of the approximated lattice results in the renormalized $\tilde{\mathbb{T}}$.

a new lattice with a quarter of the tensors of the original lattice. This decimation is iterated until there are only few tensors in the tensor traces, making the calculation of the expectation values tractable. Note that with some labeling care this procedure can be generalized to take into account the tensors of the form $\mathbb{T}^{\alpha,a}$, since a square of tensors $\mathbb{T}^{\alpha,a}, \mathbb{T}^{\beta,b}, \mathbb{T}^{\gamma,c}, \mathbb{T}^{\delta,d}$ maps to a square $\tilde{\mathbb{T}}^{\alpha,a}, \tilde{\mathbb{T}}^{\beta,b}, \tilde{\mathbb{T}}^{\gamma,c}, \tilde{\mathbb{T}}^{\delta,d}$ (A group of 4 tensors is "closed" under RG).

III. QUANTUM ROTOR MODEL

A. The quantum rotor Hamiltonian

Consider a d-dimensional lattice with N-component unit operators $\hat{n}_\alpha$ on each site. $\hat{n}_\alpha$ can be seen as describing the position of a particle constraint to move on the surface of N-dimensional unit sphere located at the site α. To each particle (or rotor) we assign a momentum $\hat{p_\alpha}$ with components $\hat{p}_{a,\alpha}$ satisfying the canonical commutation relations:

$$[\hat{n}_{a,\alpha}, \hat{p}_{b,\beta}] = i\delta_{\alpha,\beta}\delta_{a,b}. \tag{10}$$

It is convenient to define the rotor angular momentum $\hat{L}_{a,b,\alpha} = \hat{n}_{a,\alpha}\hat{p}_{b,\alpha} - \hat{p}_{a,\alpha}\hat{n}_{b,\alpha}$ and $\hat{L}_{c,\alpha} = \frac{\varepsilon_{cab}}{2}\hat{L}_{a,b,\alpha}$ so that the commutation relations become

$$\begin{aligned} [\hat{L}_{a,\alpha}, \hat{L}_{b,\beta}] &= i\varepsilon_{abc}\hat{L}_{c,\alpha}\delta_{\alpha,\beta}, \\ [\hat{L}_{a,\alpha}, \hat{n}_{b,\beta}] &= i\varepsilon_{abc}\hat{n}_{c,\alpha}\delta_{\alpha,\beta}, \\ [\hat{n}_{a,\alpha}, \hat{n}_{b,\beta}] &= 0. \end{aligned} \tag{11}$$

With the angular momentum, we can assign to each rotor a kinetic energy term, resulting in a total Hamiltonian of the form

$$H_{kin} = \sum_\alpha \frac{\hat{L}^2_\alpha}{2I} \tag{12}$$

where we assumed that each rotor has the same moment of inertia I. We obtain the Hamiltonian for the O(N) quantum rotor lattice by adding an interaction term

$$H = \sum_\alpha \frac{\hat{L}^2_\alpha}{2I} - \frac{1}{g}\sum_{\langle\alpha,\beta\rangle} \hat{n}_\alpha\hat{n}_\beta \tag{13}$$

where $\langle i, j\rangle$ is a summation over nearest neighbors. For the case $N = 2$, parametrize $\hat{n}_i = (\cos(\theta_i), \sin(\theta_i))$, and $\hat{L}_i = -i\frac{\partial}{\partial\theta_i}$ with eigenstates given by $|m_i\rangle = \frac{e^{im_i\theta_i}}{\sqrt{2\pi}}$. There are no naturally occurring quantum rotors in nature, but some systems such as antiferromagnets and superfluids can be studied through this model.

For $d > 1$ the quantum rotor model exhibits a disordered/paramagnetic phase as $g \to \infty$ for which $\langle\hat{n}_i \cdot \hat{n}_j\rangle \sim \exp(-\frac{|x_i - x_j|}{\xi})$, and an ordered phase in the limit $g \to 0$ with $\langle\hat{n}_i \cdot \hat{n}_j\rangle = C$. There is a critical g_c in which the quantum phase transition happens. In the $d = 1$ and $N \geq 3$ case, there is no phase transition; however, the $N = 2$ exhibits a phase transition but does not follow the long-distance behavior of $d > 1$. This is analogous to the Kosterlitz-Thouless transition of the classical XY model in $d = 2$. In fact, there is a mapping between the partition functions of the $O(N)$ quantum rotor and the classical $O(N)$ model [5].

B. TREG of the $O(2)$ quantum rotor model

The local Hamiltonian for the 2-dimensional $O(2)$ quantum rotor can be written as

$$H_\alpha = \frac{\hat{L}^2_\alpha}{2I} - \frac{1}{g}\overline{\sum_\beta}(\cos(\theta_\alpha)\cos(\theta_\beta) + \sin(\theta_\alpha)\sin(\theta_\beta)) \tag{14}$$

where the overline indicates summation over near neighbors of the site α. Let the physical variable of our tensor ansatz be the set of quantum numbers $\{m\}$ of $\hat{L}$. Note that the m's can take any integer value; however, for the low-energy physics we expect the lowest energy states to contribute the most. For this and numerical reasons, we will have a cutoff on the physical index of the tensors to be the lowest d-quantum numbers of angular momentum, $m_\alpha \in \{-\frac{d-1}{2}, -\frac{d-1}{2}+1, \cdots, \frac{d-1}{2}\}$. Defining $O^{\alpha,0} = \frac{\hat{L}^2_\alpha}{2I}$, $O^{\alpha,1} = \sqrt{-\frac{1}{g}}\cos(\theta_\alpha)$, and $O^{\alpha,2} = \sqrt{-\frac{1}{g}}\sin(\theta_\alpha)$, we see that we will have 3 types of tensors besides $\mathbb{T}$ in the expectation value of the Hamiltonian (Eq.9):

$$\begin{aligned} \mathbb{T}^{\alpha,0} &= \sum_k \frac{-k^2}{2I}\overline{T}^k \otimes T^k, \\ \mathbb{T}^{\alpha,1} &= \sqrt{-\frac{1}{g}}\sum_{k,k'}\langle k|\cos(\theta_\alpha)|k'\rangle\overline{T}^k \otimes T^{k'}, \\ \mathbb{T}^{\alpha,2} &= \sqrt{-\frac{1}{g}}\sum_{k,k'}\langle k|\sin(\theta_\alpha)|k'\rangle\overline{T}^k \otimes T^{k'}. \end{aligned} \tag{15}$$

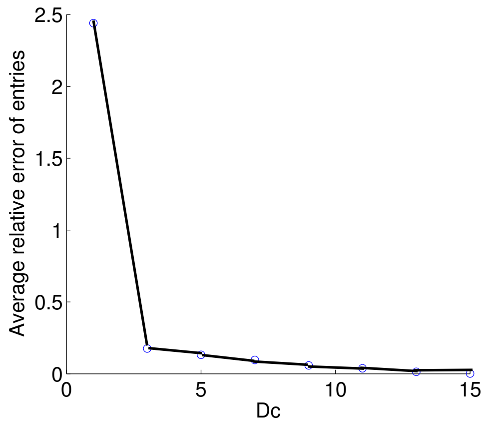

FIG. 5. A plot showing the average relative error of the entries between the approximated tensor and the actual tensor in the second step of TRG as a function of the singular value cut Dc. The black line is a piecewise linear fit.

Using $\int_0^{2\pi} \cos(\theta) e^{ik\theta} d\theta = \pi\delta_{k,\pm 1}$ and $\int_0^{2\pi} \sin(\theta) e^{ik\theta} d\theta = \pm i\pi\delta_{k,\pm 1}$, Eq. 15 becomes

$$\mathbb{T}^{\alpha,1} = \frac{1}{2}\sqrt{-\frac{1}{g}} \sum_k (\overline{T}^k \otimes T^{k+1} + \overline{T}^k \otimes T^{k-1}), \quad (16)$$
$$\mathbb{T}^{\alpha,2} = \frac{i}{2}\sqrt{-\frac{1}{g}} \sum_k (\overline{T}^k \otimes T^{k+1} - \overline{T}^k \otimes T^{k-1}).$$

This is all we need to perform the TERG method.

IV. PRELIMINARY RESULTS

We tried a TPS like the one in Eq. 2 where we let T be a real tensor with bond dimensionality $D = 2$, and with rotation by 90° symmetry. Unfortunately, the implementation is a preliminary one and may contain mistakes. Even for 6 iteration of the TRG, the SVD step breaks down due to overflow error. The current implementation lacks the minimization step which can be done with the scipy.optimize library. For a $2^3 \times 2^3$ lattice, after a 2^4 decimation (performing the TRG approximation 4 times) we obtain for a totally real tensor T an onsite energy and a bond energy of the order 10^{100}. In the future we hope to finish and increase the efficiency of the code.

To quantify the approximation done in the first step of the TERG with the singular cut value, we calculated the average relative error between the approximation tensor and the actual tensor for each entry. We started with a randomize real tensors, then calculated the average relative error of an entry by calculating the relative error between each entry and then getting the average. Repeating the process 100 times and taking another average, we found that the approximation seems fairly accurate. Results are shown in Fig. 5. It was also checked "by hand" that no particular entry relative error were far away from this average.

V. CONCLUSION

Besides TRG and TERG, many other methods based on tensor-network algorithms have been develop to study strongly correlated systems in low-dimensions such as the multiscale renormalization ansatz (MERA)[6], and linearized tensor-renormalization group (LTRG)[7]. In this paper, we discussed how tensor-renormalization techniques give us a method to study 2-dimensional quantum lattice models. However, tensor-renormalization can also be used to study 1-dimensional quantum systems through algorithms such as the tensor-entanglemente-filtering renormalization group (TEFRG) [3]. As discussed in Ref. [5], the 1-dimensional $O(2)$ quantum rotor exhibits a Kosterlitz-Thouless transition. Recent work [8] have shown that the thermodynamic properties of the classical 2-dimensional XY model as calculated with the use of tensor-renormalization agree very well with results from Kosterlitz [9], with high temperature expansions [10], and Monte Carlo calculations [11]. It is left for future work to study the Kosterlitz-Thouless transition of the $O(2)$ quantum rotor chain with the use of tensor-renormalization techniques such as TEFRG.

ACKNOWLEDGMENTS

I would like to thank Prof. Kardar for his MIT 8.334 class, as well as Tim Hsie for making me aware of the existence of the tensor-renormalization group.

[1] M. Levin and C. P. Nave, Phys. Rev. Lett. **99**, 120601 (2007).
[2] Z.-C. Gu, M. Levin, and X.-G. Wen, Phys. Rev. B **78**, 205116 (2008).
[3] Z.-C. Gu and X.-G. Wen, Phys. Rev. B **80**, 155131 (2009).
[4] S. R. White, Phys. Rev. Lett. **69**, 2863 (1992).
[5] S. Sachdev, *Quantum Phase Transitions* (Cambridge University Press, 2011).
[6] G. Vidal, Phys. Rev. Lett. **99**, 220405 (2007).
[7] W. Li, S.-J. Ran, S.-S. Gong, Y. Zhao, B. Xi, F. Ye, and G. Su, Phys. Rev. Lett. **106**, 127202 (2011).
[8] J. F. Yu, Z. Y. Xie, Y. Meurice, Y. Liu, A. Denbleyker, H. Zou, M. P. Qin, J. Chen, and T. Xiang, Phys. Rev. E **89**, 013308 (2014).
[9] J. M. Kosterlitz, Journal of Physics C: Solid State Physics **7**, 1046 (1974).
[10] H. Arisue, Phys. Rev. E **79**, 011107 (2009).
[11] M. Hasenbusch and K. Pinn, Journal of Physics A: Mathematical and General **30**, 63 (1997).